An Improvement of Convergence in Finite element Analysis with Infinite Element Using Deflation

Hiroki Ito, Kota Watanabe, and Hajime Igarashi
Graduate School of Information Science and Technology, Hokkaido University
Kita 14 Nishi 9, Kita-ku, Sapporo 060-0814, JAPAN

This paper presents a deflation technique to improve the convergence of finite element (FE) analyses with infinite elements. In FE analyses of electromagnetic fields, large air regions must be discretized into FE meshes. This leads to increases in computational time. The infinite element in which electromagnetic fields in air region are accurately expressed has been introduced in order to solve this problem. However, when using the infinite element, convergence of iterative liner solvers deteriorates because the condition number of FE matrices becomes large. In this paper, a deflation technique to improve convergence of iterative solvers is introduced. Numerical examples show that the proposed technique can improve convergence characteristics in a magnetostatic analysis with finite and infinite elements.

***Index Terms*— Electromagnetic field analysis, Finite element method, Deflation, Infinite element**

I. Introduction

In numerical analysis of electromagnetic fields, the finite element (FE) method has widely been used. Because electromagnetic fields treated in these analyses usually spread over infinite air space, the air region must be discretized into a lot of FE meshes. This leads to increases in computational time and cost of mesh generation. One of the solutions of this problem is introduction of the infinite elements (IEs) [1].

The IE is an element that consists of two types of edges: edges on the surface on FEs and edges infinitely spread in a radial manner, (see Fig. 1). The former edges are associated with FE edges so as to fit the IEs to the surface of FE. One of the advantages in use of IEs is that it can accurately express electromagnetic fields which spread infinity in air region. Hence we can reduce the number of FE meshes in air region by introducing IEs. However, there is a disadvantage in use of IEs that the condition number of FE matrices becomes large. This results in poor convergence of iterative linear solvers such as the incomplete Cholesky preconditioned conjugate gradient (ICCG) method and increases in computational times. For this reason, improvement in convergence of ICCG in FE analyses with IEs has been required so far.

One of the techniques to improve the convergence of ICCG is orthogonalization of basis functions for the IEs [2]. In this paper, we introduce another approach to improve conditioning of FE matrices using the eigenvalue deflation technique [3],[4]. The deflation technique replaces small eigenvalues of the system matrices with zeros. Therefore, the condition number of the system matrix can be improved. The deflation techniques have been applied to magnetostatic problems with flat finite elements to improve conditioning of FE matrices [3]-[5]. Moreover the deflation technique can be formulated in a different manner by introducing augmented matrices [3]. In this work, the deflation technique is applied to the Gramian matrices relevant to IEs to improve conditioning of global FE matrices. Because the Gram matrices are small and invariant over all the IEs, computational burden of the eigenvectors of the Gram is negligible. It will be shown that the present method drastically improves the number of iterations and computational times of ICCG applied to FE analysis of a magnetostatic problem.

II. Infinite Element

Let us consider the IE proposed in [1]. The IE method is based on the multi-pole expansion of potentials. The IEs are connected to usual FE on the interface between finite and infinite regions. In addition, the FE matrix relevant to the IEs is shown to be sparse and symmetric. Thus, the FE matrix constructed from usual FE and IEs can be solved by the ICCG method.

Figure 1 shows a rectangular IEs connected to a hexahedral FE. The IEs consists of four finite edges on the interface to the FE and four infinite edges whose ends are at the interfacial vertexes of the FE. The latter edges radially extend to infinity. A reference point O (X_0, Y_0, Z_0) is placed in the finite region. The local coordinate system consists of r, s and t; $-1 < r, s < 1$, $1<t < \infty$. The position vector at an arbitrary point $P(\boldsymbol{x})$ in IE is given by:

$$\boldsymbol{x} = \boldsymbol{X} + t\left(\sum_{i=1}^{4} \omega_i \boldsymbol{x}_i - \boldsymbol{X}\right). \tag{1}$$

where $\boldsymbol{X}=(X_0, Y_0, Z_0)$ denotes a reference point in the finite region, ω_i is a two-dimensional shape the rectangular FE. The explicit form of ω_i is summarized in Table I. The covariant component $\boldsymbol{e}_r$, $\boldsymbol{e}_s$, $\boldsymbol{e}_t$ and the contravariant component $\boldsymbol{e}^r$, $\boldsymbol{e}^s$, $\boldsymbol{e}^t$ relevant to the local coordinate system (r, s, t) are given by:

Manuscript received July 1, 2011. Corresponding author: H. Ito (hiroito@em-si.eng.hokudai.ac.jp).
Digital Object Identifier inserted by IEEE

$$\boldsymbol{e}_r \equiv \frac{\partial \boldsymbol{x}}{\partial r} = t\sum_{i=1}^{4}\frac{\partial \omega_i}{\partial r}\boldsymbol{x}_i = t\,\boldsymbol{e}_{r0},$$
$$\boldsymbol{e}_s \equiv \frac{\partial \boldsymbol{x}}{\partial s} = t\sum_{i=1}^{4}\frac{\partial \omega_i}{\partial s}\boldsymbol{x}_i = t\,\boldsymbol{e}_{s0}, \tag{2}$$
$$\boldsymbol{e}_t \equiv \frac{\partial \boldsymbol{x}}{\partial t} = \sum_{i=1}^{4}\omega_i\boldsymbol{x}_i,$$

$$\boldsymbol{e}^r = \nabla r = \frac{\boldsymbol{e}_s\times\boldsymbol{e}_t}{\sqrt{g}} = \frac{\boldsymbol{e}_{s0}\times\boldsymbol{e}_t}{t\sqrt{g}} = \frac{\boldsymbol{e}_0^r}{t},$$
$$\boldsymbol{e}^s = \nabla s = \frac{\boldsymbol{e}_t\times\boldsymbol{e}_r}{\sqrt{g}} = \frac{\boldsymbol{e}_t\times\boldsymbol{e}_{r0}}{t\sqrt{g}} = \frac{\boldsymbol{e}_0^s}{t}, \tag{3}$$
$$\boldsymbol{e}^t = \nabla t = \frac{\boldsymbol{e}_r\times\boldsymbol{e}_s}{\sqrt{g}} = \frac{\boldsymbol{e}_{r0}\times\boldsymbol{e}_{s0}}{\sqrt{g}},$$

where $\sqrt{g}$ denotes the Jacobian. In the IEs, the magnetic vector potential $\boldsymbol{A}$ is interpolated in the form

$$\boldsymbol{A} = \sum_{n=1}^{k}\Big(\sum_{e=1}^{8}\boldsymbol{N}_e^n A_e^n\Big), \tag{4}$$

where k is the order of the series expansion, and $\boldsymbol{N}_e^n$ is the n-th order shape function of IEs defined by,

$$\begin{aligned}\boldsymbol{N}_e^n &= \tau_n(t)(f_e(r,s)\boldsymbol{e}^r + g_e(r,s)\boldsymbol{e}^s)\\ &= \frac{\tau_n(t)}{t}\left(f_e(r,s)\boldsymbol{e}_0^r + g_e(r,s)\boldsymbol{e}_0^s\right),\end{aligned} \quad (e=1,2,3,4), \tag{5}$$

$$\boldsymbol{N}_e^n = -\frac{\partial\tau_n}{\partial t}h_e(r,s)\boldsymbol{e}^t = -\gamma_n h_e(r,s)\boldsymbol{e}^t, \quad (e=5,6,7,8). \tag{6}$$

In (5) and (6), the functions τ_n are usually chosen as $1/t^n$, $n = 1, 2, \ldots, k$ The explicit form of $f_e(r, s)$, $g_e(r, s)$ and $h_e(r, s)$ are summarized in Table II. The rotation $\boldsymbol{N}_e^n$ is given by:

$$\mathrm{rot}\boldsymbol{N}_e^n = \frac{\gamma_n(t)}{t}\boldsymbol{v}_e(r,s) + \frac{\tau_n(t)}{t^2}\boldsymbol{u}_e(r,s), \quad (e=1,2,3,4), \tag{7}$$

$$\mathrm{rot}\,\boldsymbol{N}_e^n = -\frac{\gamma_n(t)}{t}\boldsymbol{w}_e(r,s) \ (e=5,6,7,8), \tag{8}$$

where vectors $\boldsymbol{v}_e$, $\boldsymbol{u}_e$ and $\boldsymbol{w}_e$ are defined as follows:

$$\boldsymbol{v}_e(r,s) \equiv \frac{1}{\sqrt{g}}(-g_e(r)\boldsymbol{e}_{r0} + f_e(s)\boldsymbol{e}_{s0}), \tag{9}$$

$$\boldsymbol{u}_e(r,s) \equiv \frac{1}{\sqrt{g}}\left(\frac{dg_e}{dr} - \frac{df_e}{ds}\right)\boldsymbol{e}_t, \tag{10}$$

$$\boldsymbol{w}_e(r,s) \equiv \frac{1}{\sqrt{g}}\left(\frac{\partial h_e}{\partial s}\boldsymbol{e}_{r0} - \frac{\partial h_e}{\partial r}\boldsymbol{e}_{s0}\right). \tag{11}$$

The local IEs matrix $K_{ee'}^{nm}$ which is obtained from discretization of the Maxwell equation of magnetostatic fields in an air region, rot (rot $\boldsymbol{A}$) = $\mu_0\boldsymbol{J}$, is expressed as follows:

$$K_{ee'}^{nm} = \iiint \mathrm{rot}\boldsymbol{N}_e^n[g_{ij}]\mathrm{rot}\boldsymbol{N}_{e'}^m\sqrt{g}\,dr\,ds\,dt, \tag{12}$$

where $[g_{ij}]$ is a 3×3 metric tensor. The explicit form of $K_{ee'}^{nm}$ in (12) can be written in the forms

$$\begin{aligned}K_{ee'}^{nm} &= G_1\iint \boldsymbol{u}_e[g_{ij}]\boldsymbol{u}_{e'}\sqrt{g}\,dr\,ds + G_2\iint \boldsymbol{v}_e[g_{ij}]\boldsymbol{v}_{e'}\sqrt{g}\,dr\,ds\\ &\quad + G_3\iint \boldsymbol{v}_e[g_{ij}]\boldsymbol{u}_{e'}\sqrt{g}\,dr\,ds + G_4\iint \boldsymbol{u}_e[g_{ij}]\boldsymbol{v}_{e'}\sqrt{g}\,dr\,ds\end{aligned}$$
$$(1\le e, e'\le 4), \tag{13}$$

$$K_{ee'}^{nm} = G_2\iint \boldsymbol{w}_e[g_{ij}]\boldsymbol{w}_{e'}\sqrt{g}\,dr\,ds, \quad (5\le e, e'\le 8), \tag{14}$$

$$K_{ee'}^{nm} = -G_2\iint \boldsymbol{w}_e[g_{ij}]\boldsymbol{w}_{e'}\sqrt{g}\,dr\,ds - G_4\iint \boldsymbol{u}_e[g_{ij}]\boldsymbol{w}_{e'}\sqrt{g}\,dr\,ds$$
$$(1\le e\le 4,\ 5\le e'\le 8), \tag{15}$$

$$K_{ee'}^{nm} = -G_2\iint \boldsymbol{w}_e[g_{ij}]\boldsymbol{w}_{e'}\sqrt{g}\,dr\,ds - G_3\iint \boldsymbol{v}_e[g_{ij}]\boldsymbol{w}_{e'}\sqrt{g}\,dr\,ds$$
$$(5\le e\le 8,\ 1\le e'\le 4), \tag{16}$$

where the Gramian matrices G_1, G_2, G_3 and G_4 are defined as follows:

$$\begin{aligned}G_1 &= \int_1^\infty \frac{\tau_n\tau_m}{t^2}dt, \quad G_2 = \int_1^\infty \gamma_n\gamma_m dt\\ G_3 &= \int_1^\infty \frac{\gamma_n\tau_m}{t}dt, \quad G_4 = \int_1^\infty \frac{\tau_n\gamma_m}{t}dt\end{aligned}. \tag{17}$$

The condition numbers of the Gramian matrices, whose structures are like the Hilbert matrix, are significantly large. This is the reason why introduction of IEs results in poor conditioning of FE matrices. In the next section, we introduce a deflation technique to improve the conditioning of the Gramian matrices as well as the global FE matrix.

FIG. 1 HERE
TABLE 1, 2 HERE

III. Deflation Technique

We will give a brief introduction of the deflation method and then apply it to the Gramian matrix. Let us consider a system of linear equations

$$K\boldsymbol{x} = \boldsymbol{b}, \tag{18}$$

where K is an $n \times n$ symmetric semi-positive definate matrix, the vector $\boldsymbol{b}$ is assumed to be in the range of K. The eigenvalues of K are written as $\lambda_1\le\lambda_2\le\ldots\le\lambda_n$. We introduce the matrix W defined by

$$W = [\boldsymbol{w}_1, \boldsymbol{w}_2, \ldots, \boldsymbol{w}_k], \tag{19}$$

which is composed of the orthogonal eigenvectors of K, corresponding to $\lambda_1,\ldots,\lambda_k$. It is assumed that the eigenvalues

$\lambda_1,\ldots,\lambda_k$ are so small that the conditioning of K is poor. The unknown vector $\boldsymbol{x}$ is decomposed into the vector in the eigenspace spanned by the eigenvectors corresponding to small eigenvalues, $W\boldsymbol{z}$, and $\boldsymbol{y}$. The unknown vector $\boldsymbol{z}$ can be determined from the orthogonality condition $(\boldsymbol{b}-K(\boldsymbol{y}+W\boldsymbol{z}), \boldsymbol{w}_i) = 0$, that is:

$$W^t KW\boldsymbol{z} = W^t(\boldsymbol{b} - K\boldsymbol{y}) . \tag{20}$$

Moreover (18) is now written as

$$K(\boldsymbol{y} + W\boldsymbol{z}) = \boldsymbol{b} . \tag{21}$$

In [6], (20) and (21) are iteratively solved. From (20) and (21), we can obtain the modified system of equations with an augmented matrix as follows [6], [7]:

$$\begin{bmatrix} K & KW \\ W^t K & W^t KW \end{bmatrix} \begin{bmatrix} \boldsymbol{y} \\ \boldsymbol{z} \end{bmatrix} = \begin{bmatrix} \boldsymbol{b} \\ W^t \boldsymbol{b} \end{bmatrix} . \tag{22}$$

It is shown that the eigenvalues of the diagonally scaled augmented matrix in (22) are k zeros, $1+\lambda_1,\ldots,1+\lambda_k$, $\lambda_{k+1},\ldots, \lambda_n$ [3]. Hence, the conditioning of the augmented matrix in (22) is much better than that of K.

Now we apply the above mentioned deflation technique to the Gramian matrices in (17), which are represented hereafter by

$$G = <\boldsymbol{\varphi}^t, \boldsymbol{\varphi}> = \begin{bmatrix} (\varphi_1,\varphi_1) & (\varphi_1,\varphi_2) & \cdots \\ (\varphi_2,\varphi_1) & \ddots & \\ \vdots & & \end{bmatrix} , \tag{23}$$

where $\boldsymbol{\varphi} = \{\varphi_1, \varphi_2, ..., \varphi_n\}$. The $N \times k$ matrix $W_k = [\boldsymbol{w}_1, \boldsymbol{w}_2, \ldots, \boldsymbol{w}_k]$ is composed of the eigenvectors of the small eigenvalues of G, where $k \le N$. The new basis functions $\boldsymbol{\varphi}'$ are introduced with W_k as follows:

$$\boldsymbol{\varphi}' = \begin{bmatrix} I \\ W_k^t \end{bmatrix} \boldsymbol{\varphi} , \tag{24}$$

where I denotes the unit matrix, namely, the new basis functions are given by

$$\boldsymbol{\varphi}' = [\varphi_1, \varphi_2, \ldots, \varphi_n, \boldsymbol{w}_1^t\boldsymbol{\varphi}, \boldsymbol{w}_2^t\boldsymbol{\varphi}, \ldots, \boldsymbol{w}_k^t\boldsymbol{\varphi}]^t . \tag{25}$$

Note that the additional bases are linearly dependent functions, which are introduced to improve the conditioning of G. The Gramian matrix for the new bases can be obtained by substituting (24) into (23), that is,

$$\tilde{G} = <\boldsymbol{\varphi}', \boldsymbol{\varphi}'^t> = \begin{bmatrix} G & GW_k \\ W_k^t G & W_k^t G W_k \end{bmatrix} . \tag{26}$$

The augmented matrix in (26) corresponds to that in (23). The preconditioned matrix $\tilde{G}$ is expected to have better conditioning in comparison with G. Because the ill conditioning of the global FE matrix constructed with the IE method is originated from the large condition number of G, the present method would improve the conditioning of the global FE matrix.

The structure of the deflated global FE matrix K_{def} is shown Fig. 2, where the K_{F} is a usual FE matrix, the K_{I} is the matrix relevant to IEs and the K_{DI} is the deflated infinite matrix. The components corresponding to the IEs in the right hand vector $\boldsymbol{b}$ are usually zero, because the region in IE is air region. Hence, no special treatments are required for $\boldsymbol{b}$.

FIG. 2 HERE

IV. Numerical Result

We apply the present method to a simple magnetostatic field problem to verify its effectiveness. Figure 3 shows a three dimensional model which consists of a coil and air region. The numbers of FEs and IEs are 21660 and 28808, respectively and the order of IE is set to 4 in this analysis.

Table III summarizes the condition number of G_1 with the deflation based on $W_{1k} = [\boldsymbol{w}_{11}, \boldsymbol{w}_{12},\ldots, \boldsymbol{w}_{1k}]$, where $\boldsymbol{w}_{ij}$ denotes the j-th eigenvector of the Gramian matrix G_i. Note that the condition number is computed after the matrix is preconditioned with the diagonal scaling. We can see that the condition number rapidly decreases as the order of deflation increases.

The convergence histories of ICCG applied to the FE equation with the conventional and the deflated FE matrices are shown in Fig. 4. This result indicates that the convergence ICCG is significantly improved by using the present method, and the improvement becomes more evident when the order k of deflation increases.

The convergence characteristics can be changed when using the eigenvectors of other Gramian matrix in (17). To test this, we also employ the matrix $W_{2k} = [\boldsymbol{w}_{21}, \boldsymbol{w}_{22},\ldots, \boldsymbol{w}_{2k}]$ constructed from G_2 for the present method. Table IV summarizes the iteration counts and CPU times when we use W_{1k} and W_{2k} for deflation. It is found that the convergence with W_{2k} is better than that with W_{1k}. Furthermore, it can be seen that the combination of W_{11} and W_{21} has the best performance. In the view of CPU time, reduction in the number of iterations does not always bring the good performance, because the number of unknowns increases when using the present method.

Finally we investigate the error of the solution by introducing the IEs, In order to show clearly the influence of the air region size on the solution, we analyze a simple model which consists of a line current with $0.05\times0.05\mathrm{mm}^2$ and air region. Fig. 5 shows the dependency on inductance. We can see that the inductance obtained by using IEs is not affected by decrease in the region size and is in good agreement with that obtained by the FE analysis with enough air region size.

FIG. 3, 4, 5 HERE

TABLE 3, 4 HERE

V. Conclusion

In this paper, we have introduced a definition technique for infinite elements to improve the matrix conditioning. The deflation technique is applied to the Gramian matrix relevant to the infinite elements. The present method is applied to a magnetostatic analysis using the finite and infinite elements. It is shown that the condition number of Gramian matrix becomes small by the deflation. Numerical examples show that the convergence of ICCG applied to FE analysis based on the infinite elements is improved significantly using the present method.

References

[1] S. Tamitani, T. Takamatsu, A. Otaka, S. Wakao, A. Kameari and Y. Takahashi, "Finite-Element Analysis of Magnetic Field Problem With Open Boundary Using Infinite Edge Element," *IEEE Trans. Magn.*, vol. 47, no 5, pp.1194-1197, May. 2011.

[2] S. Taminani, et al, "Orthogonalized Infinite Edge Element Method – Convergence Improvement by Orthogonalization of Hilbert Matrix in Infinite EdgeElement Method–," to be presented at COMPUMAG2011, submitted to *IEEE Trans. Magn*.

[3] H. Igarashi, K .Watanabe, "Deflation techniques for computational electromagnetism: theoretical consideration," *IEEE Trans. Magn.*, vol.47, no.5, pp.1438-1441, 2011.

[4] C. Vuik, A. Segal, J.A. Meijerink, "An efficient preconditioned CG method for the solution of a class of layered problems with extreme contrasts in the coefficients," J. Comp. Phys., vol.152, pp.385-403, 1999.

[5] H. De Gersem, K. Hameyer, "A deflated iterative solver for magnetostatic finite element models with large differences in permeability," Eur. Phys. J. AP., vol.13, no.1, pp.45-49, 2001.

[6] T. Mifune, S. Moriguchi, T. Iwashita, M. Shimasaki, "Convergence acceleration of iterative solvers for the finite element analysis using the implilcit and explicit error correction methods," *IEEE Trans. Magn.*, vol.45, no.3, pp.1104-1107, 2009.

[7] A. Kameari, "Improvement of ICCG convergence for thin elements in magnetic field analyses using the finite-element method," *IEEE Trans. Magn.*, vol.44, no.6, pp.1178-1181, 2008.

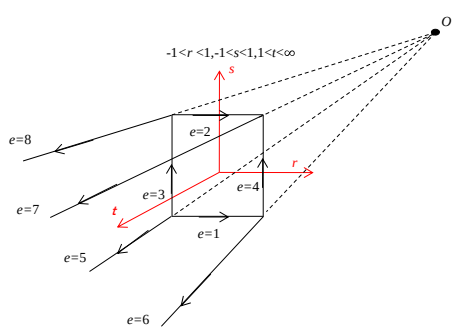

Fig. 1. Local coordinates of infinite element

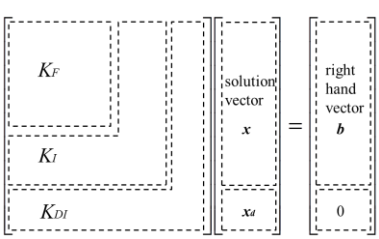

Fig. 2. Deflated full coefficient matrix

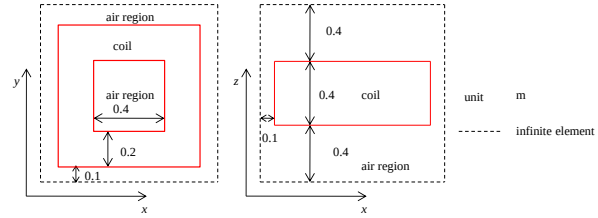

Fig. 3. Analysis coil model

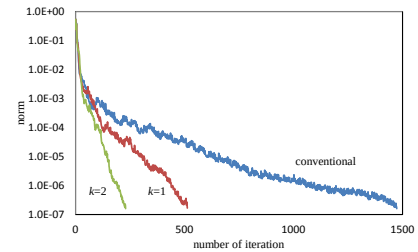

Fig. 4. Convergence history

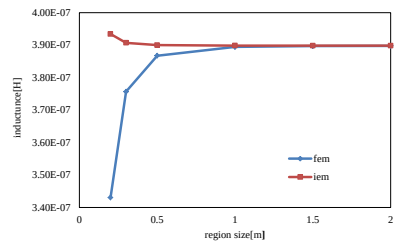

Fig. 5. influence of air region size on inductance

TABLE I
Explicit form of ω_i

node number i	ω_i
1	(1-r)(1-s)/4
2	(1+r)(1-s)/4
3	(1+r)(1+s)/4
4	(1-r)(1+s)/4

TABLE II
Explicit form of (5) and (6)

edge number e	$f_e(r,s)$	$g_e(r,s)$	edge number e	$h_e(r,s)$
1	(1-s)/4	0	5	(1-r)(1-s)/4
2	(1+s)/4	0	6	(1+r)(1-s)/4
3	0	(1-r)/4	7	(1+r)(1+s)/4
4	0	(1+r)/4	8	(1-r)(1+s)/4

TABLE III
Condition number of augmented matrix G_1 with w11

number of deflation k	condition number
without deflation	9.5×10^4
1	1.0×10^3
2	2.5×10
3	3.8

TABLE IV
Number of iteration and CPU time

method*	number of unknowns	number of iteration	CPU time[s]
without deflation	50468	1474	68
$G_1(1)$	57670	513	31.0
$G_1(2)$	64872	230	15.6
$G_1(3)$	72074	189	16.9
$G_2(1)$	57670	314	23.14
$G_2(2)$	64872	126	10.1
$G_1(1)$, $G_2(1)$	64872	116	8.55

*The numbers in the parentheses represent k, which is the number of vectors $\boldsymbol{w}_{ij}$ for deflation.